Published OnlineFirst August 11, 2009; DOI: 10.1158/1535-7163.MCT-09-0347

Induction of endoplasmic reticulum stress response by TZD18, a novel dual ligand for peroxisome proliferator-activated receptor α/γ, in human breast cancer cells

Chuanbing Zang,[1] Hongyu Liu,[1] Janina Bertz,[1] Kurt Possinger,[1] H. Phillip Koeffler,[2] Elena Elstner,[1] and Jan Eucker[1]

[1]Division of Oncology/Hematology, University Medicine (Charité), Berlin, Germany and [2]Division of Hematology/Oncology, Cedars-Sinai Medical Center/UCLA, School of Medicine, Los Angeles, California

Abstract

Previously we reported that the peroxisome proliferator-activated receptor α/γ dual ligand TZD18 inhibited growth and induced apoptosis of leukemia and glioblastoma cells. Now we show that TZD18 also has the same effects against six human breast cancer cell lines. To obtain insights into the mechanism involved in TZD18-induced growth inhibition and apoptosis in breast cancer, the gene expression profiles of TZD18-treated and untreated MCF-7 and MDA-MB-231 cells were compared by microarray analysis. Results reveal that many genes implicated in endoplasmic reticulum stress signaling, such as *CHOP* (also known as *DDIT3* or *GADD153*), *GRP78* (*HSPA5*), and *ATF4*, are highly up-regulated, suggesting endoplasmic reticulum stress is induced. This is supported by our data that treatment of MCF-7 and MDA-MB-231 cells with TZD18 induces phosphorylation of PERK and the α subunit of eukaryotic initiation factor 2 (eIF2α), as well as an up-regulation of GRP78 and an activation of ATF6, all of which are specific markers for endoplasmic reticulum stress. Furthermore, this ligand increases the endoplasmic reticulum stress–related cell death–regulators such as CHOP, DR5, GADD34, Bax, and Bak in these cells. Importantly, knockdown of CHOP by small interference RNA antagonizes the TZD18-induced apoptosis, indicating a crucial role of CHOP in the apoptotic process triggered by TZD18. In addition, TZD18 also activates stress-sensitive mitogen-activated protein kinase (MAPK) pathways including p38, ERK, and JNK. The specific inhibitors of these MAPKs attenuated the TZD18-induced growth inhibition in these cells. These results clearly show that activation of these MAPKs is important for TZD18-induced growth inhibition. In summary, TZD18-treatment leads to the activation of endoplasmic reticulum stress response and, subsequently, growth arrest and apoptosis in breast cancer cells. [Mol Cancer Ther 2009;8(8):2296–307]

Introduction

The family of peroxisome proliferator-activated receptors (PPAR), which belongs to nuclear hormone receptors, is involved in a wide range of biological processes such as adipocyte differentiation, glucose and lipid homeostasis and inflammation (1–3). Current evidence indicates that the γ isoform of this family (PPARγ) is also prominently expressed in a variety of human cancers and its activation by its specific agonists such as members of thiazolidinedione (TZD) antidiabetic drugs or its natural-occurring ligand 15-deoxy-$\Delta^{12,14}$ prostaglandin J_2 leads to growth inhibition, cellular differentiation, and/or apoptosis of these malignant cells (4, 5). We showed previously that PPARγ is expressed in human breast cancer cell lines and fresh breast adenocarcinomas. Importantly, PPARγ agonist troglitazone (TGZ), either alone or in combination with all-trans retinoic acid, irreversibly inhibits cancer cell growth and induces significant apoptosis in various human breast cancer cell lines mediated by a bcl-2–dependent pathway (6, 7). Furthermore, TGZ, either alone or together with all-trans retinoic acid, also strongly inhibits MCF-7 tumor growth in a nude murine model without significant side effects to the mice (6). In agreement with our results, evidence from other groups also indicated that a variety of PPARγ agonists repress the growth and induce differentiation and apoptosis of various breast cancer cells (8, 9). Furthermore, mutations of PPARγ in either breast cancer cell lines or in the patient's breast tumor samples were not detectable (10), indicating that somatic mutations in the PPARγ gene are rare events in breast carcinoma. These observations make PPARγ a promising target for breast cancer therapy.

Notably, many of the published *in vitro* studies utilized concentrations of TZDs higher than those typically used for activation of PPARγ. Therefore, for comparable effects *in vivo*, a relatively high local concentration of TZDs is required around the tumor tissues. Thus, the classic antidiabetic TZDs

Received 11/7/08; revised 4/14/09; accepted 5/1/09; published OnlineFirst 8/11/09.

Grant support: This work was supported by the grants (to E. Elstner.) from the "Berliner Krebsgesellschaft e.V.", Deutsche Forschungsgemeischaft, and the "Deutsche José Carreras Leukämie-Stiftung e.V." H.P. Koeffler is supported by NIH grants, the Parker Hughes Fund, and the C. and H. Koeffler Foundation.

The costs of publication of this article were defrayed in part by the payment of page charges. This article must therefore be hereby marked *advertisement* in accordance with 18 U.S.C. Section 1734 solely to indicate this fact.

Note: C. Zang, H. Liu, E. Elstner, and J. Eucker contributed equally to this manuscript.

Requests for reprints: Chuanbing Zang, Department of Hematology and Oncology, Charité Campus Mitte, Universitätsmedizin Berlin, Charitéplatz 1, 10117 Berlin, Germany. Phone: 0049-30-450513253; Fax: 0049-30-450513950. E-mail: chuanbing.zang@charite.de

doi:10.1158/1535-7163.MCT-09-0347

Published OnlineFirst August 11, 2009; DOI: 10.1158/1535-7163.MCT-09-0347

might not be the best candidates for their anticancer applications. Instead, novel and more potent PPAR ligands should be developed specifically for their anticancer effects.

Recently, several novel dual PPARα/γ ligands have been synthesized by Merck (USA) with extremely high potential to activate both PPARγ and PPARα, another member of the PPAR superfamily. Studies have revealed that PPARα is expressed in cancer cells (11, 12), and PPARα ligands inhibit the growth of several types of cancer cells (13, 14). These data led us to hypothesize that the dual ligands for PPARα/γ might be even more effective in inhibiting cancer cell growth than ligands for either PPARγ or PPARα alone. Indeed, we found that TZD18 (12), one of these dual ligands, exhibits more potent antigrowth activity than conventional antidiabetic TZDs against human glioblastomas (15) and bcl-abl positive leukemia cells (12, 16).

The mechanism underlying the anticancer effects of TZDs has not been fully elucidated. Recent studies have reported that conventional TZDs could induce endoplasmic reticulum stress in human lung cancer cells (17). The endoplasmic reticulum is the primary site of synthesis, posttranslational modification, and folding of secreted and membrane-bound proteins. Endoplasmic reticulum stress is elicited when proteins are either unfolded or misfolded due to certain stimuli and accumulate in the endoplasmic reticulum. Endoplasmic reticulum stress activates a set of signaling pathways known as the unfolded protein response (UPR). UPR is mediated by three transmembrane receptors: pancreatic endoplasmic reticulum kinase-like endoplasmic reticulum kinase (PERK), activating transcription factor 6 (ATF6), and inositol-requiring enzyme 1 (IRE1). These three "sensor" proteins each initiate signaling cascades that promote protein folding via up-regulation of endoplasmic reticulum protein chaperones and reduce the accumulation of unfolded proteins via inhibition of general protein translation (18). UPR is a cellular protective response against various stresses. However, if the unfolded protein accumulation is persistent and the stress cannot be relieved, UPR signaling switches from prosurvival to proapoptotic (19, 20). One of the major mediators of the proapoptotic signaling of endoplasmic reticulum stress is the transcriptional factor CHOP (also known as GADD153), which initiates either death receptor–related extrinsic and/or bcl-2 family–involved intrinsic apoptotic pathways.

In this study, we showed for the first time that treatment of human breast cancer cells with TZD18 resulted in induction of growth arrest and apoptosis which is coupled to the endoplasmic reticulum stress response.

Materials and Methods

Materials

TZD18 was kindly provided by Merck. Kinase inhibitors U0126, PD098059, SP600125, and SB203580 were purchased from Merck. All these compounds were dissolved at 10^{-2} mol/L in DMSO and stock solutions were stored at −80°C and further diluted to appropriate concentrations with medium before use. Specific caspase inhibitors (Z-VAD-FMK, Z-LEHD-FMK, and Z-IETD-FMK) were purchased from R&D Systems. Stock solutions (20 mmol/L) were made in DMSO and stored at −80°C.

Cell Lines and Cell Culture

The human breast cancer cell lines MCF-7, MDA-MB-231, MDA-MB-436, BT-20, SKBR-3, and BT474 were purchased from the American Type Culture Collection (ATCC) and maintained in DMEM supplemented with 10% FCS and 1% penicillin/streptomycin. Cells in logarithmic growth phase were used for experiments.

Flow Cytometry

Cells were treated with different concentrations of TZD18 for different durations, washed with PBS, and fixed with ice-cold 70% ethanol. These samples were treated with RNase, stained with propidium iodide, and analyzed with the FACSCalibur flow cytometer (Becton Dickinson).

Proliferation and Terminal Deoxynucleotidyl-transferase-mediated UTP Nick End Labeling Assays

Cell proliferation was evaluated using conventional MTT [3-(4,5-dimethylthiazol-2-yl)-2,5-diphenyl tetrazolium bromide] assay as previously described (21). Apoptosis was determined by terminal deoxynucleotidyl-transferase-mediated UTP nick end labeling (TUNEL) technique using an *in situ* cell death detection kit (Roche Applied Biosystems) following the instructions of the manufacturer.

Microarray Analysis

Either MCF-7 or MDA-MB-231 cells were cultured in 6-well culture plates for 24 h either with or without TZD18 (30 μmol/L). Total RNA was extracted using the RNeasy Mini Kit (Qiagen). Biotin-labeled cRNA probes were generated from 10 μg RNA for each condition and hybridized to HU-U133A Genechip expression arrays (Affymetrix) according to the manufacturer's protocols. Hybridization data were analyzed with GeneSpring software version 7.0 (Silicon Genetics). Only measurements with a raw value of ≥10 were used. Raw data were normalized and genes were selected as TZD18-regulated genes if their expression changed ≥2-fold as compared with the cells without treatment.

Western Blot Analysis

Protein concentrations of cell lysates were measured using the BCA protein assay kit (Pierce). Western blot analysis was done as described previously (21). The following antibodies were from Santa Cruz: anti-CHOP, anti-GADD34, anti-GRP78, anti-p-PERK, anti-ATF6, anti-p21, anti-p-JNK, anti-JNK, anti-Bax, anti-Bak, and anti-β-actin. The following antibodies were from Cell Signaling: anti-p-eIF2α, anti-p-p38, anti-p38, anti-p-p42/44 MAPK, and anti-p42/44 MAPK. Anti-DR5 was purchased from Abcam. Horseradish peroxidase–labeled antimouse IgG, antirabbit IgG, and antigoat IgG from Santa Cruz were used as secondary antibodies. Primary antibodies were diluted from 1:200 to 1:1,000.

Detection of XBP-1 Splicing by Reverse Transcription-PCR

Reverse transcription-PCR (RT-PCR) reactions were carried out with GeneAmp PCR system 2700 (Applied

Published OnlineFirst August 11, 2009; DOI: 10.1158/1535-7163.MCT-09-0347

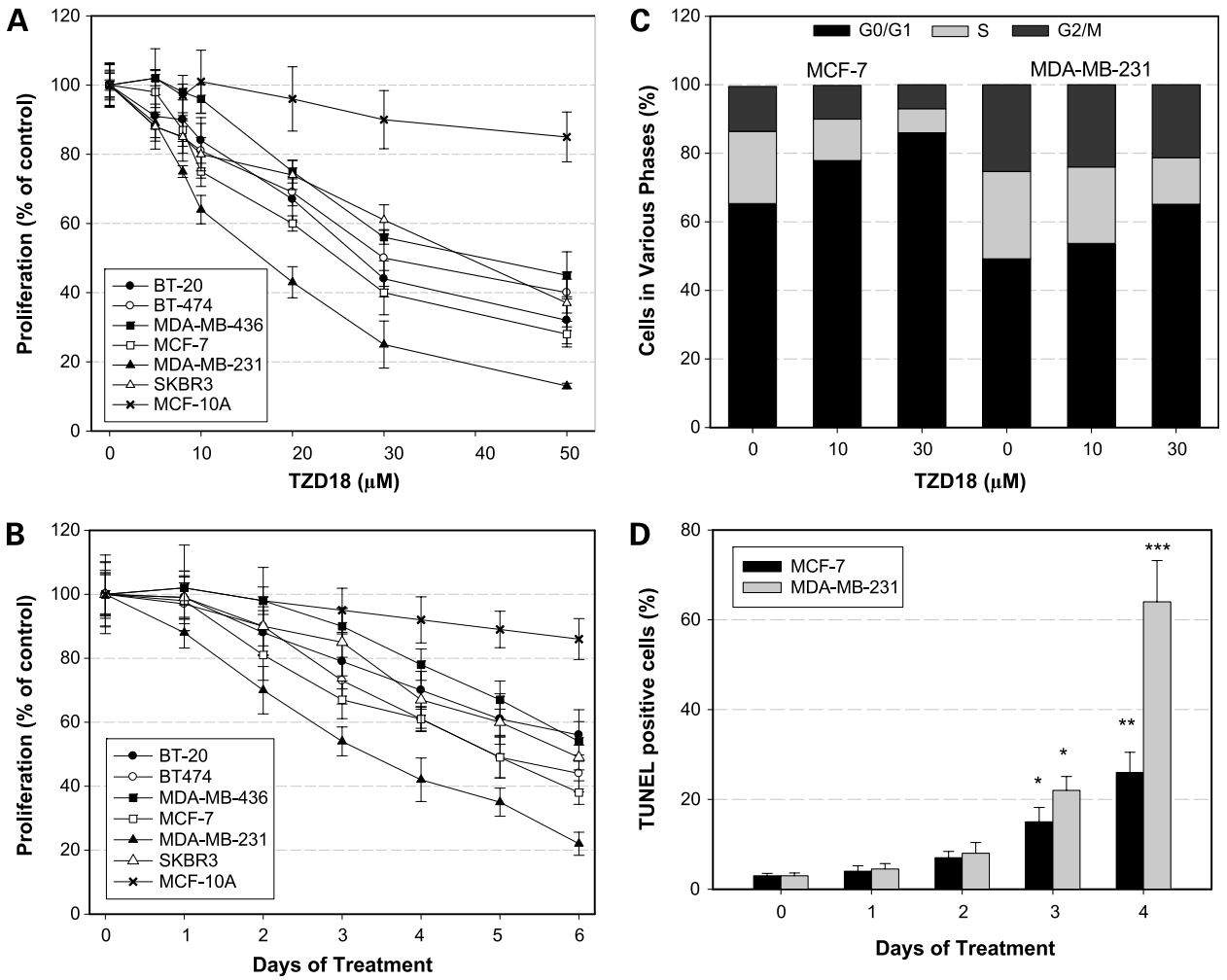

Figure 1. Inhibitory effects of TZD18 in a variety of human breast cancer and normal breast cell lines. **A**, dose-dependent growth inhibition of TZD18 in breast cancer or normal cell lines. Cells were treated with TZD18 at different concentrations for 6 d. Cell proliferation was determined by MTT assay. Results were expressed as percentage of control (without treatment). Values are mean ± SD of six parallel experiments. **B**, time-dependent growth inhibition by TZD18 in a variety of breast cancer or normal cell lines. Cells were treated with TZD18 (30 μmol/L) for different durations. Cell proliferation was determined by MTT assay. Results were expressed as percentage of control (without treatment). Values are mean ± SD of six parallel experiments. **C**, alteration of cell cycle distribution of MCF-7 and MDA-MB-231 cells by TZD18. Cells (2×10^5) were incubated either in the presence or absence of TZD18 (10 or 30 μmol/L) for 3 d, fixed, treated with RNase, and stained for DNA with propidium iodide. Cell cycle distribution was determined by flow cytometry. Results represent the percentage of the total cell population. Figure is representative of three independent experiments. **D**, induction by TZD18 of apoptosis of both MCF-7 and MDA-MB-231 cells. Cells (2×10^4) were incubated either in the presence or absence of TZD18 (30 μmol/L) for different durations. Apoptotic cells were measured by TUNEL assay as described in Materials and Methods. TUNEL-positive cells were counted and results were expressed as percentage of total counted cells. Data represent the mean ± SD of triplicate experiments. *, $P < 0.05$; **, $P < 0.01$; ***, $P < 0.001$ as compared with untreated controls.

Biosystem). RNA extraction and cDNA preparation were described previously (21). Following reverse transcription, 1 μL cDNA was used for further PCR analysis. The sequences of primers for XBP-1 and PCR conditions were adapted from Lin JH et al. (22). The sequences were: forward: 5′-ttacgagagaaaactcatggc; reverse: 5′-gggtccaagttgtccagaatgc. Both unspliced (XBP-1U) and spliced (XBP-1S) XBP-1 mRNA fragments would be amplified.

Detection of Caspase Activities by Colorimetric Caspases Activity Assay Kits

The activities of caspase-3, -8, and -9 in the cells that were untreated or treated with TZD18 were determined with colorimetric caspases activity assay kits (Chemicon) according to the manufacturer's recommendations. Briefly, 2×10^6 cells were lysed in lysis buffer, and the protein concentration for each sample was measured using the BCA protein assay kit. Incubation of cell lysates with caspase-specific substrates led to cleavage of these substrates by corresponding caspases, and release of chromophore p-nitroaniline. The caspase activities were detected by measuring this chromophore using the Anthos HTII ELISA reader at 405 nm. Optical density values were then normalized to protein concentrations of the samples. Fold-increase in caspase activities before and after TZD18 treatment was determined

Published OnlineFirst August 11, 2009; DOI: 10.1158/1535-7163.MCT-09-0347

by comparing the optical density value of the TZD18-treated sample with that of untreated control.

Transfection of Small Interference RNA

Knockdown of CHOP, PPARα, or PPARγ was carried out by transfection of small interference RNA (siRNA). The siRNA against human *CHOP* (si CHOP), *PPARα* (si PPARα), and *PPARγ* (si PPARγ), as well as their negative control siRNA (si Control), were purchased from Ambion. Transfection was done using LipofectAMINE 2000 (Invitrogen). Briefly, breast cancer cells were plated in a 6-well plate at 3×10^5 cells/well at day 1. At day 2, cells were washed and incubated for 6 h with 500 μL of siRNA and LipofectAMINE 2000 mixture following the general transfection procedure provided by manufacturer. This was followed by the addition of 1.5 mL growth media to each well and cultured for an additional 24 h. Cells were then used for Western blot analysis and MTT test in either the absence or presence of TZD18.

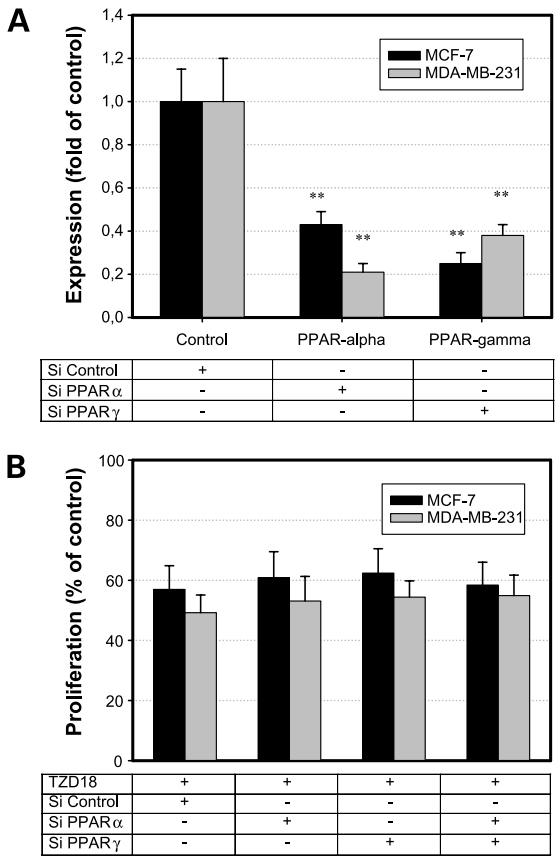

Figure 2. TZD18-induced growth inhibition is independent of PPAR-α and PPAR-γ. MCF-7 and MDA-MB-231 cells were transfected with control (scrambled) siRNA or siRNAs against either PPARα or PPARγ. **A**, expression of PPARα and PPAR-γ in transfected cells was quantified by real-time RT-PCR. Results were expressed as fold of control cells transfected with Scramble siRNA (si Control). Mean ± SD of triplicate experiments are shown. **B**, siRNA-transfected cells were incubated with TZD18 (30 μmol/L) for 3 d. Cell proliferation was measured by MTT assay. Because the siRNA transfection technique does not itself affect cell growth, results were normalized as a percentage of control cells, which were transfected with scrambled siRNA but not treated with TZD18. Data are expressed as percentage of control and are the mean ± SD of six parallel experiments. **, $P < 0.01$ as compared with control siRNA–transfected samples.

Quantitative (Real-time) RT-PCR

The quantification of the mRNA levels of PPARα and PPARγ was assayed using SYBR Green two-step real-time RT-PCR. Twenty microliters of cDNA were synthesized from 1 μg of total RNA from each sample as described (21). PCR amplification was done in triplicates using QuantiTect SYBR Green PCR kit (Qiagen) according to the instruction of manufacture in an ABI Prism 7700 sequence detection system. β-Actin was also amplified from the same sample as an endogenous control using the predeveloped Taqman assay for human β-actin (Applied Biosystems). Primers used for PPARα and PPARγ were adapted from Suchanek et al. (11) and Melichar et al. (23), respectively. The sequences of the primers were: PPARα sense: 5′-GCTGGTGCAGATCATCAAGAAG-3′ and antisense: 5′-GGTGTGGCTGATCTGAAGGAA-3′; PPARγ sense: 5-GGCTTCATGACAAGGGAGTTTC-3 and antisense: 5-AACTCAAACTTGGGCTCCATAAAG-3. PCR products were quantified using $\Delta\Delta C_T$ method and normalized to actin as described (21).

Statistical Analysis

The experiments were repeated at least twice. Each experiment was done at least in triplicates. The results are expressed as mean ± SD. Statistical analyses were done by Student's *t*-test and $P < 0.05$ was considered as statistically significant.

Results

TZD18 Caused Growth Inhibition in Breast Cancer Cells

Treatment of breast cancer cells with TZD18 resulted in dose- and time-dependent growth inhibition in breast cancer cell lines (Fig. 1A and B). Proliferation of each of the cell lines was inhibited in a time- and dose-dependent fashion. Cell growth began to decrease after 2 days of culture. Interestingly, the MDA-MB-231 cell line, a highly aggressive and metastatic cell line, was most sensitive to TZD18. The concentration of TZD18 that inhibited 50% proliferation (IC_{50}) was around 18 μmol/L after 6 days of incubation. The IC_{50} of other cell lines was between 25 and 40 μmol/L. We have previously shown that TZD18 had no inhibitory effects on human CD34-positive hematopoietic stem cells at these concentrations (16). In agreement with this observation, we showed here that the normal MCF-10A cells were relatively resistant to the TZD18-induced growth inhibition (Fig. 1A and B), suggesting that the observed inhibitory effects on human breast cancer cells is not due to nonspecific cytotoxicity of TZD18. Importantly, the growth inhibitory effect of TZD18 on human breast cancer cells was much stronger than that of conventional TZDs such as pioglitazone (PGZ) and TGZ. The IC_{50} of TZD18 on MDA-MB-231 and MCF-7 cell lines were 18 μmol/L and 25 μmol/L, respectively, after 6 days of culture. Under the same conditions, the IC_{50} of PGZ was >50 μmol/L for both cell lines whereas the IC_{50} of TGZ was around 45 μmol/L and 36 μmol/L, respectively (data not shown). Because MDA-MB-231 and

Published OnlineFirst August 11, 2009; DOI: 10.1158/1535-7163.MCT-09-0347

Table 1. List of genes involved in UPR and induced by TZD18 treatment in either MCF-7 or MDA-MB-231 cells

Gene name	Genbank	Description	Fold change	
			MDA-MB-231	MCF-7
GDF15	AF003934	Growth differentiation factor 15	17.67	15.29
DDIT3	BC003637	DNA-damage-inducible transcript 3 (CHOP/GADD153)	3.37	12.39
DDIT4	NM_019058	DNA-damage-inducible transcript 4	3.21	10.35
HSPA1A	NM_005345	Heat shock 70 kDa protein 1A	7.37	2.37
GADD45A	NM_001924	Growth arrest and DNA-damage-inducible, α	5.1	6.14
CDKN1A	NM_000389	Cyclin-dependent kinase inhibitor 1A (p21, Cip1)	1.7	6.13
HSPA1B	NM_005346	Heat shock 70 kDa protein 1B	4.23	1.28
TNFRSF-10B (DR5)	AF016266	Tumor necrosis factor receptor superfamily, member 10 b (death receptor 5, DR5)	2.3	4.12
ATF3	NM_001674	Activating transcription factor 3	2.56	3.58
HERPUD1	AF217990	Homocysteine-inducible, endoplasmic reticulum stress-inducible, ubiquitin-like domain member 1	2.89	4.99
HSPA5	AF216292	Heat shock 70 kDa protein 5 (glucose-regulated protein, 78 kDa)	2.68	2.79
ATF4	NM_001675	Activating transcription factor 4 (tax-responsive enhancer element B67)	2.4	2.45

NOTE: MCF-7 and MDA-MB-231 cells were treated with TZD18 (30 μmol/L) for 24 h. After incubation, total RNA was isolated and applied to microarray analysis as described in Materials and Methods. Genes that changed ≥2-fold in their expression levels by TZD18 were selected using GeneSpring software. Several genes that closely related to endoplasmic reticulum stress signaling are listed.

MCF-7 cells were the two cell lines that were most sensitive to TZD18, we chose these two cell lines for further studies.

To determine whether TZD18-induced inhibition of cell growth was related to cell cycle arrest and/or apoptosis, we initially analyzed the cell cycle distribution of either MCF-7 or MDA-MB-231 cells after a 3-day culture with TZD18 because we began to notice a significant growth arrest at that time point. In each case, an accumulation of cells in G_0-G_1 phase occurred with a decrease of the S-phase (Fig. 1C). The alterations of cell cycle distribution were negligible before the 2-day exposure to TZD18 and became significant only after 3 days of culture with TZD18 (data not shown). In addition, TZD18 caused significant apoptosis of both MCF-7 and MDA-MB-231 cells as determined by TUNEL assay (Fig. 1D) after 4 days of culture with TZD18. MDA-MB-231 cells were, again, more sensitive to TZD18-induced apoptosis than were MCF-7 cells. Consistent with the cell cycle and cell proliferation data, apoptosis became evident only after 3 days of exposure to TZD18. In contrast to breast cancer cells, TZD18 did not induce obvious apoptosis of normal MCF-10A cells (data not shown).

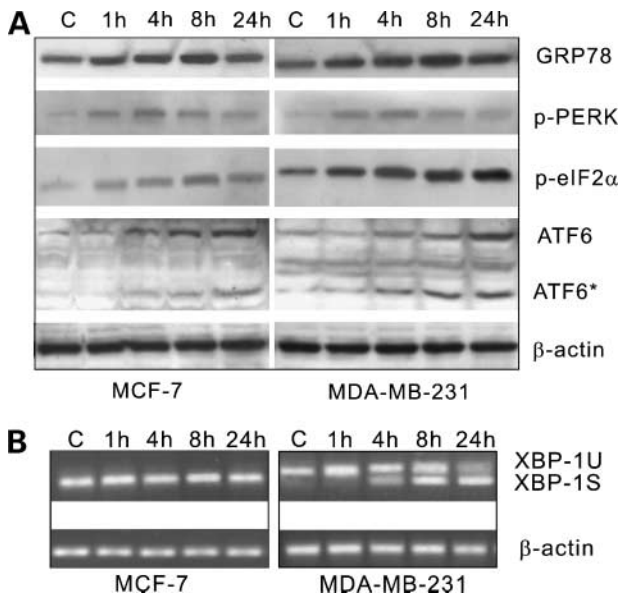

Figure 3. Induction of endoplasmic reticulum stress sensor proteins by TZD18 in MCF-7 and MDA-MB-231 cells. **A**, cells were stimulated with TZD18 (30 μmol/L) for different durations as indicated. Cell lysates were prepared, and equal amounts (30 μg) of total proteins were subjected to Western blot analysis. GRP78, phospho-PERK, phospho-eIF2α, and ATF6 were detected. β-Actin was the loading control. ATF6* was the activated form of ATF6. **B**, in order to detect XBP-1 splicing, MCF-7 or MBA-MB-231 cells were treated with TZD18 (30 μmol/L) for different durations as indicated. Total RNA was isolated and 1 μg of RNA was used to generate cDNAs by reverse transcription. PCR was carried out using XBP-1 specific primers. XBP-1 splicing was shown by the appearance of spliced XBP-1 product. XBP-1S, spliced XBP-1; XBP-1U, unspliced XBP-1.

Growth Inhibition Induced by TZD18 was Independent of PPARα and PPARγ

We have previously shown that the PPARα and PPARγ antagonists could not reverse the TZD18-induced growth inhibition of human bcr-abl positive leukemia cells (12, 16). In this study, we decreased the expression of either PPARα or PPARγ in MCF-7 and MDA-MB-231 cells by small RNA interference. Transfection of siRNA alone had no obvious effects on cell proliferation (data not shown). As expected, transfection of siRNA specifically against PPARα and PPARγ significantly repressed the expression of PPARα and PPARγ. As shown in Fig. 2A, transfection of siRNA against PPARα into MCF-7 or MDA-MB-231 cells reduced their expression of PPARα up to 60% and 80% of control (scrambled) siRNA, respectively. Similarly, transfection of siRNA against PPARγ into either MCF-7 or MDA-MB-231 cells diminished their expression of PPARγ by 75% and 60% as compared with control siRNA–transfected

Published OnlineFirst August 11, 2009; DOI: 10.1158/1535-7163.MCT-09-0347

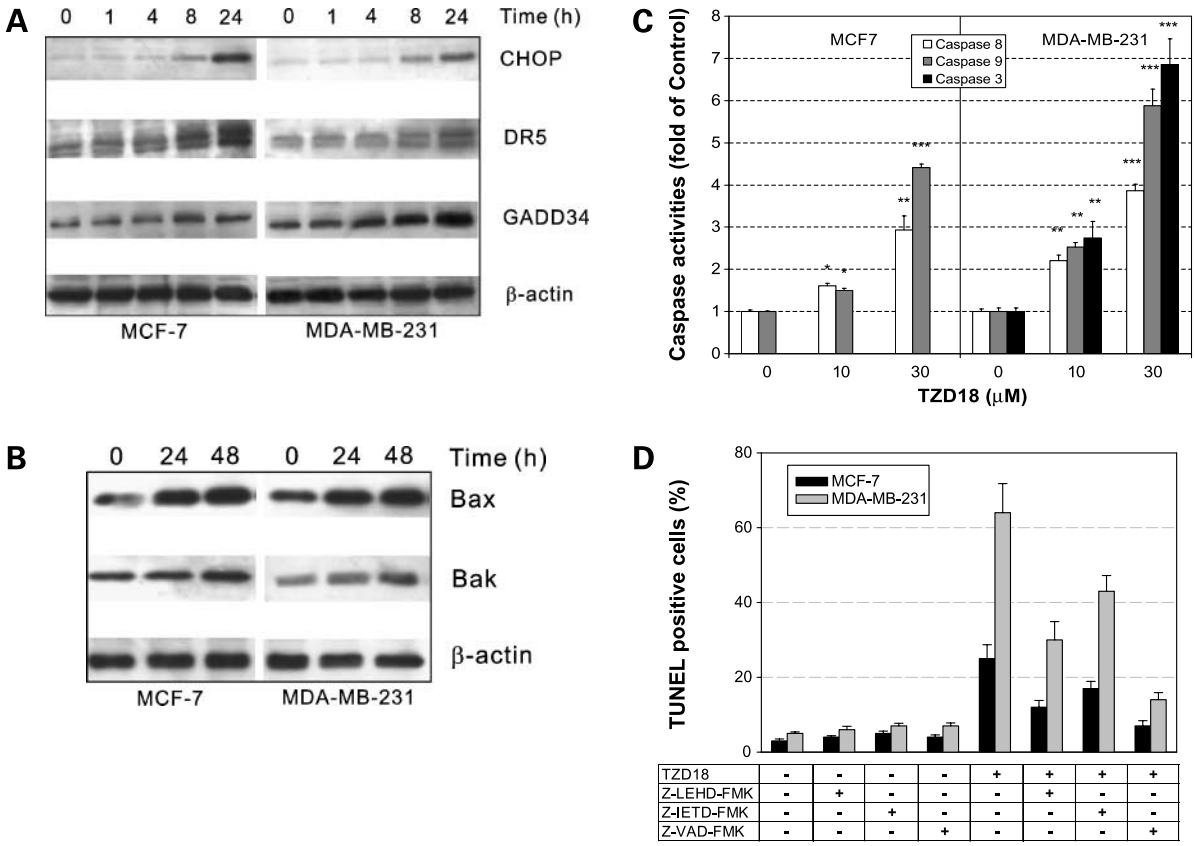

Figure 4. Induction of endoplasmic reticulum stress–associated apoptosis by TZD18 in MCF-7 and MDA-MB-231 cells. **A**, cells were stimulated with TZD18 (30 μmol/L) for different durations as indicated. Cell lysates were prepared, and equal amounts (30 μg) of total proteins were subjected to Western blot analysis using specific antibodies against CHOP/GADD153, DR5, and GADD34. β-Actin served as a loading control. Representative blots of three independent experiments are shown. **B**, cells were stimulated with TZD18 (30 μmol/L) for 24 and 48 h. Cell lysates were analyzed by immunobloting using specific antibodies against Bax and Bak. β-Actin served as loading control. Representative blots of three independent experiments are shown. **C**, cells were cultured either in the presence or absence of TZD18 (10 or 30 μmol/L) for 4 d, washed, and lysed in lysis buffer. Caspase-8, -9, and -3 activities in the cell lysates were measured as described in Materials and Methods. Results are expressed as fold increase of optical density values compared with control (without treatment). Data are expressed as mean ± SD of triplicate experiments. *, $P < 0.05$; **, $P < 0.01$; ***, $P < 0.001$ as compared with untreated cells. **D**, cells were cultured in the presence of either TZD18 (30 μmol/L), pan-caspase inhibitor Z-VAD-FMK (20 μmol/L), caspase 9 inhibitor Z-LEHD-FMK (20 μmol/L), caspase 8 inhibitor Z-IETD-FMK (20 μmol/L), or their combinations for 4 d. Apoptosis was examined using TUNEL assay as described in Materials and Methods. Apoptosis was indicated by percentage of TUNEL-positive cells in total counted cells. Results are the mean ± SD of three individual experiments.

cells, respectively. The knockdown of these mRNAs could be easily detected up to 4 days after the transfection (data not shown). Although the expression of PPARα and/or PPARγ was strongly reduced by appropriate siRNA, the antigrowth effects of TZD18 could not be blocked by these siRNAs in either MCF-7 or MDA-MB-231 cells (Fig. 2B). These results strongly suggest that the TZD18 exerts its antigrowth effects mainly through a mechanism independent of PPAR-α and PPAR-γ.

Endoplasmic Reticulum Stress–related Genes Were Altered by TZD18

We were very interested in the mechanism underlying the anticancer effects of TZD18, especially the early events triggered by TZD18 that lead to growth inhibition. Therefore, gene expression profiles of MCF-7 and MDA-MB-231 cells were generated either in the absence or presence of TZD18 (30 μmol/L) for 24 hours. Analysis by GeneSpring software revealed that the expression of >1,500 genes was changed ≥2-fold in TZD18-treated MCF-7 and MDA-MB-231 cells. We noted that many of the genes that are related to endoplasmic reticulum stress and its downstream signaling were highly up-regulated by TZD18 (Table 1). These included chaperone *GRP78* (glucose-regulated protein, 78 kDa, also called *HSPA5* or *BiP*), *DDIT3* (DNA-damage-inducible transcript 3, also called *CHOP* or *GADD153*), *XBP-1* (x-box binding protein 1), and *ATF-3* and *-4* (activating transcription factor 3 and 4). The regulation of these endoplasmic reticulum stress–related genes by TZD18 strongly suggested that TZD18 may induce UPR in these cells.

TZD18 induced UPR in Human Breast Cancer Cells

Given the well-established role of GRP78, PERK, eukaryotic initiation factor 2α (eIF2α), ATF6, and IRE1 in UPR, we examined the expression of these UPR-associated proteins

Published OnlineFirst August 11, 2009; DOI: 10.1158/1535-7163.MCT-09-0347

Table 2. Caspase activities in cell lysates treated with TZD18 (30 μmol/L) for different durations

Cell lines	Caspases	Days of treatment			
		1	2	3	4
MCF-7	Caspase 8	1.2 ± 0.2	1.8 ± 0.3	2.2 ± 0.3	3.1 ± 0.4
	Caspase 9	1.1 ± 0.1	1.5 ± 0.2	3.2 ± 0.4	4.4 ± 0.5
	Caspase 3	N.D.	N.D.	N.D.	N.D.
MDAMB-231	Caspase 8	1.1 ± 0.1	2.0 ± 0.3	2.8 ± 0.3	3.9 ± 0.5
	Caspase 9	1.2 ± 0.1	1.8 ± 0.2	3.7 ± 0.4	5.8 ± 0.4
	Caspase 3	1.0 ± 0.1	1.3 ± 0.1	4.6 ± 0.3	6.9 ± 0.6

NOTE: Cells were cultured either in the presence or absence of TZD18 (30 μmol/L) for different durations, washed, and lysed in lysis buffer. Caspase-8, caspase-9, and caspase-3 activities in the cell lysates were measured as described in Materials and Methods. Results are expressed as fold increase of optical density values compared with control (without treatment). Data are expressed as mean ± SD of triplicate experiments.
Abbreviation: N.D., not detectable.

before and after TZD18 treatment for different duration in human breast cancer cells by Western blot. Because UPR is an early cellular response to endoplasmic reticulum stress, we analyzed the expression of these proteins at 1 to 24 hours of treatment with TZD18. GRP78 was up-regulated within 1 hour after the addition of TZD18 in both MCF-7 and MDA-MB-231 cells (Fig. 3A). In addition, TZD18 enhanced the phosphorylation of PERK and its downstream target eIF2α in both MCF-7 and MDA-MB-231 cells, indicating that PERK was activated by TZD18 in these cells. Furthermore, ATF6 was also up-regulated and further processed to a 50-KDa short form as early as 4 hours after TZD18 treatment in both cell lines (Fig. 3A). In contrast, we did not observe these changes when the cells were treated with PGZ (data not shown). Interestingly, no obvious changes of these proteins were observed when the normal MCF-10A cells were treated with the same concentrations of TZD18 (data not shown).

During periods of endoplasmic reticulum stress, activated IRE1 cleaves XBP1, resulting in synthesis of a highly active transcription factor that stimulates the transcription of chaperone genes such as *GRP78* and *GRP94*. In order to evaluate the activities of IRE1, we studied the splicing of XBP-1 by RT-PCR. A splicing of XBP-1 mRNA was observed as early as 4 hours after addition of TZD18 to MDA-MB-231 cells (Fig. 3B), suggesting that IRE1 was activated by TZD18 in these cells. In contrast, TZD18 did not induce splicing of XBP-1 in MCF-7 cells (Fig. 3B).

TZD18 Enhanced the Accumulation of Endoplasmic Reticulum Stress–induced Apoptotic Proteins

PERK, ATF6, and IRE1 can also trigger proapoptotic signals when stress conditions persist. The proapoptotic signaling is mainly mediated by induction of CHOP and, possibly, its downstream components such as GADD34, death receptor 5 (DR5), and bcl-2 family proteins (20, 24). We found that expression of CHOP was induced as early as 8 hours after addition of TZD18 (30 μmol/L) in both MCF-7 and MDA-MB-231 cells (Fig. 4A), which paralleled the induction of DR5 (Fig. 4A). GADD34 was also moderately up-regulated by TZD18 (Fig. 4A). Although in some cell lines CHOP repressed the expression of bcl-2 (25), we did not observe a down-regulation of bcl-2 by TZD18 in either cell line (data not shown). Instead, TZD18 up-regulated the proapoptotic Bax and Bak (Fig. 4B).

TZD18 Activated Caspases in Human Breast Cancer Cells

Activation of a variety of caspases by UPR has been reported. We found that treatment of MCF-7 and MDA-MB-231 cells with TZD18 increased caspase-8 and -9 activities in both cell lines and caspase-3 only in MDA-MB-231 cells (Fig. 4C). MCF-7 cells are caspase-3–deficient because of a deletion of exon 3 of caspase-3 gene (26). Time-response experiments showed that the caspase-9 and -8 activation occurred by 48 hours of exposure to TZD18, and the caspase activities increased in a time-dependent fashion (Table 2). Activation of caspase-8 and -9 occurred almost at the

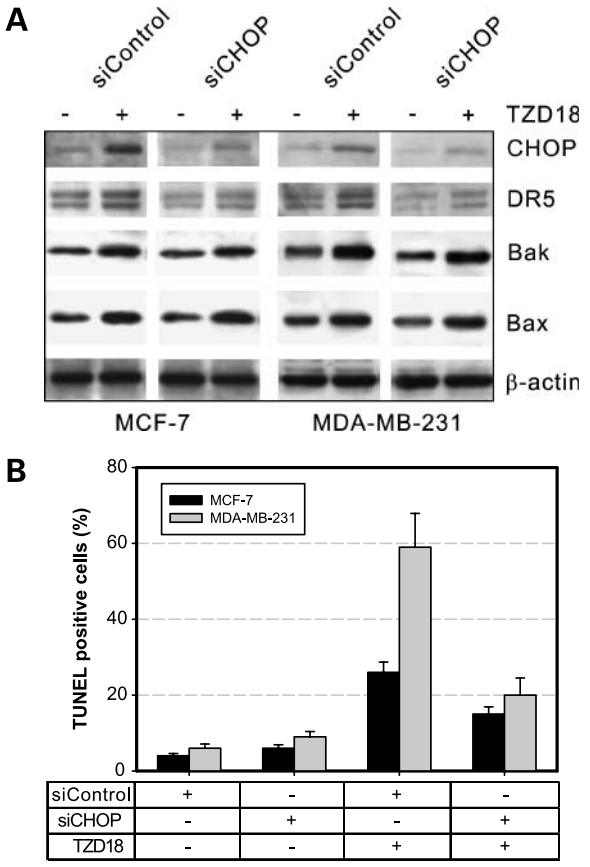

Figure 5. Knockdown of CHOP expression by siRNA reduced the TZD18-induced apoptosis of MCF-7 and MDA-MB-231 cells. Cells were transfected with control (scrambled) siRNA (si Control) or siRNA against CHOP (si CHOP). **A**, transfected cells were treated with TZD18 for an additional 24 h. Expression of CHOP, DR5, Bax, and Bak was examined using Western blot analysis with appropriate antibodies. β-Actin served as a loading control. **B**, transfected cells were incubated either with or without TZD18 (30 μmol/L) for 4 d. Apoptosis was assayed by TUNEL assay. Percentage of TUNEL-positive cells is shown. Results are the mean ± SD of triplicate experiments.

Published OnlineFirst August 11, 2009; DOI: 10.1158/1535-7163.MCT-09-0347

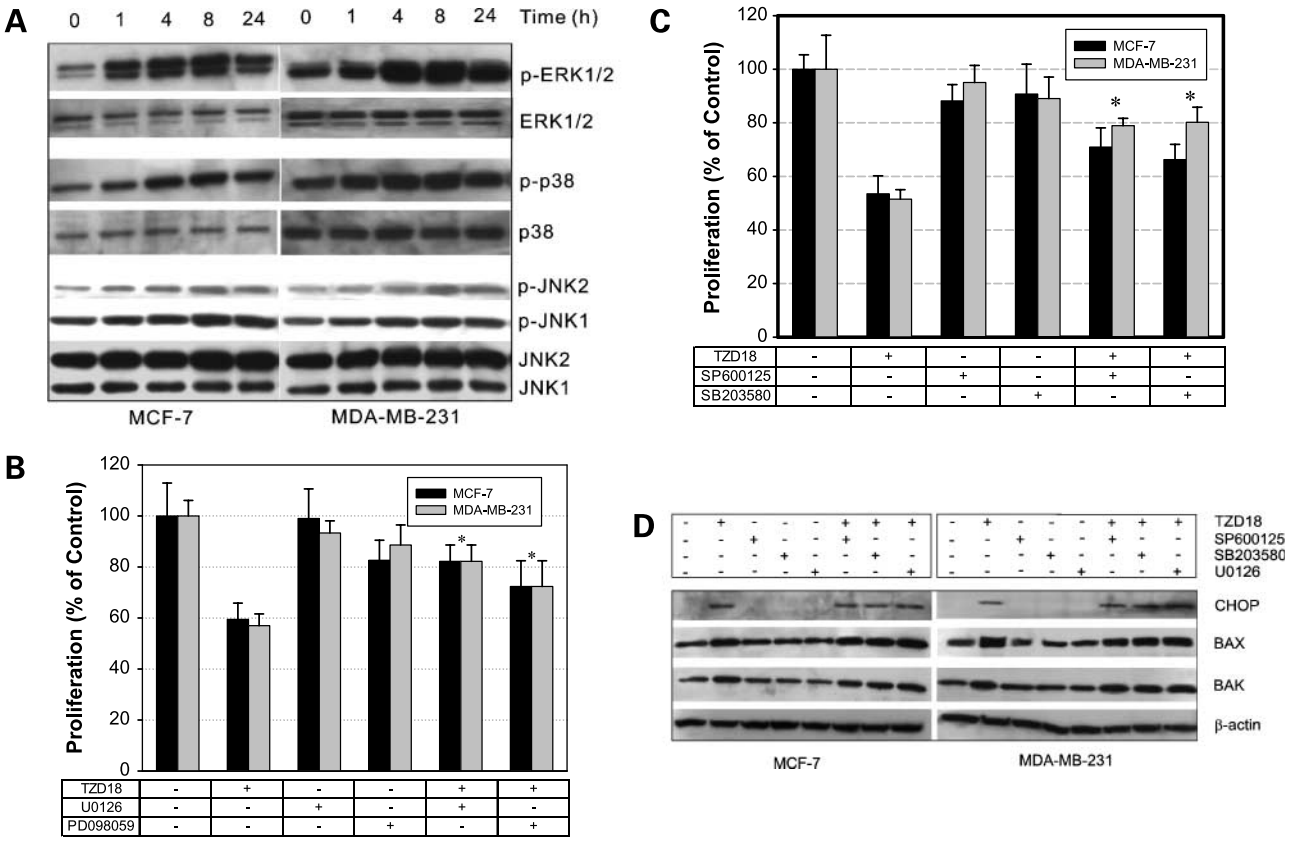

Figure 6. Treatment of MCF-7 and MDA-MB-231 cells with TZD18-induced activation of ERK, p38, and JNK. **A**, cells were treated with TZD18 (30 μmol/L) for the durations as indicated. Cell lysates were examined by Western blot with specific antibodies for phosphorylated ERK (p-ERK), total ERK, phosphorylated p38 MAPK (p-p38), total p38 MAPK, phosphorylated JNK (p-JNK1 and 2), and total JNK (JNK1 and 2). **B**, cells were incubated in the presence of either TZD18 (30 μmol/L), MEK/ERK inhibitors (1 μmol/L of U0126 or 30 μmol/L of PD098059), or both for 4 d. Cell growth was examined using MTT assay as described in Materials and Methods. Results were expressed as percentage of control (without treatment). Values are mean ± SD of six parallel experiments. *, $P < 0.05$ as compared with cells treated with TZD18 alone. **C**, cells were incubated in the presence of either TZD18 (30 μmol/L), JNK, or p38 inhibitors (1 μmol/L of SP600125 or 5 μmol/L of SB203580) or their combinations for 4 d. Cell growth was examined using MTT assay. Results were expressed as percentage of control (without treatment). Values are mean ± SD of six parallel experiments. *, $P < 0.05$ as compared with cells treated with TZD18 alone. **D**, cells were treated with either TZD18 (30 μmol/L), MAPK inhibitors (1 μmol/L of SP600125, 5 μmol/L of SB203580, or 1 μmol/L of U0126), or both for 24 h. Cell lysates were examined by Western blot with specific antibodies for CHOP, Bax, and Bak. β-Actin served as a loading control.

same time and preceded the activation of caspase-3. A close correlation between the time course of activation of caspase-8 and -9 and apoptosis induced by TZD18 suggested that caspase-8 and -9 may be involved in the TZD18-induced apoptosis. In addition, the pan-caspase inhibitor Z-VAD-FMK completely inhibited TZD18-induced apoptosis in MCF-7 and MDA-MB-231 cells (Fig. 4D), indicating that TZD18-induced apoptosis in human breast cancer cells is caspase-dependent. Furthermore, the addition of specific inhibitors for either caspase-9 (Z-LEHD-FMK) or caspase-8 (Z-IETD-FMK) partially attenuated the TZD18-induced apoptosis, further suggesting an involvement of both caspase-8 and caspase-9 in the apoptotic process initiated by TZD18 (Fig. 4D).

Involvement of CHOP in TZD18-induced Apoptosis

In order further to clarify the contribution of CHOP in TZD18-induced apoptosis, we utilized the RNA interference approach to knockdown endogenous CHOP and analyzed its effects on TZD18-induced apoptosis of MCF-7 and MDA-MB-231 cells. Transfection of CHOP siRNA strongly decreased the up-regulation of CHOP induced by TZD18 as compared with the negative control siRNA in both MCF-7 cells and MDA-MB-231 cells (Fig. 5A). Knockdown of CHOP could be detected up to 4 days after transfection of siRNA (data not shown). Interestingly, TZD18-induced DR5 expression was also antagonized by CHOP knockdown whereas the up-regulation of Bak and Bax was not attenuated by CHOP siRNA. As expected, transfection of siRNA against CHOP partially attenuated the TZD18-mediated apoptosis of both MCF-7 and MDA-MB-231 cells (Fig. 5B).

TZD18 Activated Several MAPKs in Human Breast Cancer Cells

The mitogen-activated protein (MAP) kinase (MAPK) pathway plays an essential role in a variety of cellular processes. Prior reports showed that several MAPKs such as ERK1/2, p38 MAPK, and c-Jun NH_2-terminal kinase (JNK) were activated during endoplasmic reticulum stress and either positively or negatively regulated endoplasmic

Published OnlineFirst August 11, 2009; DOI: 10.1158/1535-7163.MCT-09-0347

reticulum stress–initiated cell death (27, 28). Therefore, we investigated the effects of TZD18 on the activation (phosphorylation) of ERK, p38, and JNK by Western blot. Phosphorylation of ERK, p38, and JNK was induced by 1 hour and reached a maximum at 8 hours of exposure to TZD18 (Fig. 6A). To determine the role of activation of these MAPKs in the TZD18-induced growth inhibition of human breast cancer, the MCF-7 and MDA-MB-231 cells were treated with TZD18 in the presence of specific inhibitors of MEK/ERK (U0126, PD098059), p38 MAPK (SB203580), and JNK (SP600125). The concentrations that inhibited at least 50% of the activity of each of the kinases were chosen according to the data sheet provided by the manufacturer. After 4 days of culture, cell proliferation was assayed using the MTT assay. U0126 and PD098059, as well as SB203580 and SP600125 showed no obvious cytotoxicities to either MCF-7 or MDA-MB-231 cells (Fig. 6B and C). However, these inhibitors antagonized the growth inhibitory activity of TZD18 (Fig. 6B and C), suggesting that MEK/ERK, p38, and JNK were involved in the growth inhibitory activities of TZD18. In order to decipher whether these MAPKs regulate the TZD18-induced growth arrest through an involvement of up-regulation of CHOP and/or Bak/Bax, we blocked the MAPK activities by using specific inhibitors of these MAPKs and assessed their effects on up-regulation of CHOP and/or Bak/Bax in the presence of TZD18. As indicated in Fig. 6D, these MAPK inhibitors did not prevent the CHOP and Bak/Bax up-regulation induced by TZD18. Therefore, the molecular mechanism by which the activated MAPKs inhibited cell growth seems not to be through a direct participation in up-regulation of CHOP and Bak/Bax.

Discussion

We have shown previously that TZD18, a novel dual PPARα/γ ligand that structurally belongs to the TZD family of compounds, showed strong anticancer effects against human leukemia and glioblastoma cells (12, 15, 16). In this study, we present data showing that TZD18 also inhibited the growth of a variety of human breast cancer cell lines associated with induction of cell cycle arrest and apoptosis. These TZD18-elicited effects were much stronger than those of conventional TZDs such as PGZ and TGZ. Therefore, TZD18 represents a promising therapeutic agent for PPAR ligand-based breast cancer therapy.

By using antagonists for PPARα and PPARγ, we previously showed that activation of PPARα and PPARγ was not required for TZD18 to exert its effects on human leukemia cells (12, 16). Here, we show that knockdown of expression of PPARα and/or PPARγ by siRNA had only minimal effects on the TZD18-induced growth inhibition of both MCF-7 and MDA-MB-231 cells. These results strongly suggest that TZD18 inhibited the growth of breast cancer cells through its "off-target" effects. In order to obtain insight into the mechanisms involved in the antigrowth effects of TZD18, especially the upstream events leading to cell cycle arrest and apoptosis induced by TZD18, we analyzed the gene expression profiles before and after treatment with TZD18 for 24 hours in MCF-7 and MDA-MB-231 cells using Affymetrix microarray and GeneSpring analysis. A great number of stress-induced genes were highly up-regulated by TZD18 in both cell lines, including several typical endoplasmic reticulum stress–related genes such as *GRP78, XBP-1, CHOP, ATF-3*, and *ATF-4*. These data strongly suggested that TZD18 induced endoplasmic reticulum stress response.

In response to a range of cytotoxic stimuli, proteins are not properly folded, leading to accumulation of unfolded or misfolded proteins in the endoplasmic reticulum. Under this stress-related condition, cells elicit UPR with the aims to attenuate protein synthesis to prevent further accumulation of proteins, to induce chaperone synthesis to promote protein folding, and to induce cellular apoptosis to eliminate the stressed cells. In order to achieve these purposes, UPR initiates three types of signaling through endoplasmic reticulum transmembrane proteins, namely, PERK, ATF6, and IRE1 (18). Under physiologic conditions, these endoplasmic reticulum sensor proteins are kept in an inactive state through an association with the endoplasmic reticulum chaperone GRP78. Under conditions of stress, GRP78 disassociates from PERK, ATF6, and IRE1, and binds to unfolded proteins to promote protein folding. The disassociation of GRP78 results in activation of these endoplasmic reticulum sensors. Activated PERK phosphorylates eIF2α, leading to an inhibition of general protein synthesis and cell cycle arrest. Activated IRE1 cleaves XBP1, resulting in synthesis of a highly active transcription factor that stimulates the transcription of chaperone genes such as *GRP78* and *GRP94* and other genes that support cell survival under stress conditions. Activated ATF6 traffics to Golgi and is processed to its short form that serves as a transcription factor to induce transcription of XBP-1 and other target genes.

In this study, TZD18 enhanced the expression of GRP78, a general marker of UPR, indicating that TZD18 indeed triggered UPR in human breast cancer cells. TZD18 treatment activated all three endoplasmic reticulum sensor proteins, namely PERK, ATF6, and IRE1, in MDA-MB-231 cells. In addition to phosphorylation of PERK and its downstream target eIF2α, TZD18 also induced up-regulation and cleavage of ATF6. Furthermore, splicing of XBP-1 mRNA was also induced by TZD18 in MDA-MB-231 cells. Splicing of XBP-1 is catalyzed by activated IRE1 (29). In MCF-7 cells, we did not observe splicing of XBP-1, but we did notice an up-regulation of the endoplasmic reticulum chaperone GRP78 after treatment with TZD18. Interestingly, GRP78 is regulated by the transcription factor encoded by the spliced XBP-1 mRNA (30) as well as ATF6 (31). Also, GRP78 has been reported to be up-regulated by PERK-eIF2α (32). Phosphorylation of eIF2α by PERK, on the one hand, attenuates general protein translation, and on the other, up-regulates the expression of the ATF4 transcription factor, which, in turn, stimulates expression of *GRP78* gene and regulates its translation. Based on these published reports, TZD18 probably increases expression of GRP78 through an ATF6- and/or ATF4-dependent mechanism. We, indeed, observed an up-regulation of ATF4 in our microarray analysis and up-regulation and activation (cleavage) of ATF6

Published OnlineFirst August 11, 2009; DOI: 10.1158/1535-7163.MCT-09-0347

using Western blotting in MCF-7 cells. The observed difference in XBP-1 splicing between the MCF-7 and MDA-MB-231 cell lines is interesting and remains to be clarified. This may reflect a difference between these two cell lines to tolerate endoplasmic reticulum stress. The MDA-MB-231 cells may be sensitive to TZD18-induced endoplasmic reticulum stress and may rapidly initiate IRE1-XBP-1 signaling of UPR with the aim to protect the cells under the stress conditions. The IRE1-XBP-1 axis normally has prosurvival activity. However, when the endoplasmic reticulum stress is persistent, activated IRE1 can initiate apoptosis through recruitment of the TNF receptor associated factor 2 (TRAF2) and apoptosis signal-regulating kinase-1 (ASK1; refs. 19, 20). ASK1 is an enzyme that specifically activates a cascade leading to activation of JNK and p38 and, consequently, cell apoptosis (19, 20). We, indeed, observed an activation of JNK and p38 after addition of TZD18 to the cells. The IRE1-XBP1 axis likely exerted additional proapoptotic effects on MDA-MB-231 cells as we observed in this study.

As mentioned, endoplasmic reticulum stress response can lead to apoptosis when the conditions of endoplasmic reticulum stress persist. The major mediator of endoplasmic reticulum stress elicited apoptosis is CHOP (19, 20). *CHOP* is one of the highly induced genes during endoplasmic reticulum stress, and the PERK-eIF2α-ATF4 branch of UPR plays an essential role. *CHOP* is a direct target gene of ATF4 (33). Our microarray analysis showed that ATF4 and CHOP were up-regulated by TZD18. It is not surprising that we observed a strong time-dependent up-regulation of CHOP protein by TZD18. Studies have clearly shown that the endoplasmic reticulum stress–induced apoptosis parallels the up-regulation of CHOP (34, 35). Furthermore, CHOP knockout embryonic fibroblasts are resistant to endoplasmic reticulum stress–induced apoptosis (36). Also, forced overexpression of CHOP caused cell cycle arrest and apoptosis (37, 38). Taken together, these data show a crucial role of CHOP in apoptotic signaling initiated by UPR.

In this study, we showed that silencing of CHOP by RNA interference in either MCF-7 or MDA-MB-231 cell lines partially attenuated the TZD18-induced apoptosis. These data indicate a role of CHOP in the TZD18-induced apoptosis in human breast cancer cells. The incomplete repression of TZD18-induced apoptosis by siRNA against CHOP suggests additional CHOP-independent mechanisms may be involved in the TZD18-induced apoptosis.

CHOP belongs to the C/EBP family of transcription factors. Studies examining the target genes of this transcription factor revealed several possible downstream molecules that may be involved in CHOP-mediated apoptotic signaling. One is DR5 (24). Activation of DR5 by a variety of agents resulted in apoptosis of various human cancer cells in a CHOP-dependent manner (39, 40). Here, we noted that expression of DR5 was induced by TZD18, which occurred in parallel with the induction of CHOP. Knockdown of CHOP by siRNA also led to attenuation of DR5 expression. Therefore, we believe that induction of DR5 by TZD18 is CHOP-dependent. In addition, activation of caspase 8 after addition of TZD18 occurred in a time-dependent manner that paralleled the activation of caspase 9, suggesting that activation of caspase 8 and 9 were concurrent events. Inhibition of caspase 8 attenuated the TZD18-induced apoptosis, indicating an involvement of caspase 8, the featured caspase for the extrinsic apoptosis. Based on these results, we hypothesized that activation of DR5 death receptor may be involved in the TZD18-induced apoptosis of human breast cancer cells through the extrinsic apoptotic pathway. Further studies are required to provide more detailed evidence to confirm this hypothesis.

The other downstream molecules of CHOP signaling are the bcl-2 family members. Others have shown that CHOP can repress the expression of bcl-2 (25), and overexpression of bcl-2/bcl-xl can inhibit endoplasmic reticulum stress–induced apoptosis (41). In this study, however, expression of bcl-2 was not altered but the Bax and Bak proteins were up-regulated by TZD18. The Bak/Bax proteins have also been shown to be present in the endoplasmic reticulum membrane and are involved in endoplasmic reticulum stress–induced intrinsic apoptosis (42). Double knockout of Bak/Bax in murine embryonic fibroblasts conferred resistance to endoplasmic reticulum stress, and reconstitution of Bak in these cells restored their sensitivity to endoplasmic reticulum stress–induced apoptosis (42). In addition, we showed in this study that caspase 9, a key caspase that mediates intrinsic apoptotic signaling, was activated and involved in the apoptosis induced by TZD18. Therefore, the Bak/Bax associated intrinsic apoptotic pathway may also be involved in the TZD18-induced cell death of human breast cancer cells. CHOP knockdown by small RNA interference did not attenuate the up-regulation of Bax and Bak, suggesting that up-regulation of Bax and Bak by TZD18 was CHOP-independent. This could explain why CHOP knockdown could only partially repress the apoptosis triggered by TZD18.

A variety of MAPK cascades are activated during endoplasmic reticulum stress and have essential roles in endoplasmic reticulum stress–induced apoptosis. The most studied signaling cascade is ASK1-MAPK. ASK1 is activated under endoplasmic reticulum stress conditions and initiates activation (phosphorylation) of p38 MAPK and JNK (43). Activated p38 MAPK and JNK may positively participate in the endoplasmic reticulum stress–induced growth arrest and apoptosis by a variety of mechanisms such as transcriptional modification of CHOP (44, 45) and members of bcl-2 family (20). In this study, activation of p38 MAPK and JNK was transiently enhanced by TZD18. Moreover, specific pharmacologic inhibitors of p38 and JNK attenuated the TZD18-induced growth inhibition. These data suggest that both p38 MAPK and JNK were positively involved in the TZD18-initiated growth arrest. In order to determine whether these kinases participated in the TZD18-induced growth inhibition through a direct involvement of up-regulation of either CHOP, Bax, or Bak, we did Western blot analysis using cells treated with either TZD18 and/or the specific inhibitor of p38 and JNK. In contrast to several published studies (44, 45), these inhibitors did not

Published OnlineFirst August 11, 2009; DOI: 10.1158/1535-7163.MCT-09-0347

prevent the up-regulation of CHOP, Bax, and Bak induced by TZD18, indicating that TZD18-induced expression of CHOP, Bax, and Bak is independent of JNK and p38 MAPK. Therefore, in response to TZD18, p38 MAPK and JNK might either exert their effects on cells independent of CHOP and Bak/Bax, or act on downstream events of CHOP and Bak/Bax signaling. Our data further suggested that up-regulation of CHOP in response to endoplasmic reticulum stress stimuli by JNK and p38 MAPK may be cell type- and/or stimuli-specific.

It has been shown that stress-activated JNK and p38 MAPK could also participate in cell growth and apoptosis by phosphorylation of mitochondrial proapoptotic and antiapoptotic proteins such as Bid, Bim, and Bad, and modulate cell-cycle regulators such as CDC25, $p16^{ink4a}$, and $p19^{arf}$ (46, 47). Investigation of the roles of these molecules in TZD18-induced growth inhibition is certainly helpful to identify the mechanisms by which p38 MAPK and JNK regulate the TZD18-induced apoptosis and growth arrest in human breast cancer cells.

In addition to JNK and p38 MAPK, we found that phosphorylation of ERK was also enhanced by TZD18. Targeting the MEK/ERK pathway with either chemical inhibitors or siRNAs can reduce endoplasmic reticulum stress–induced cell death in neuroblastoma (48) and lung carcinoma cells (49). Likewise, we have also found that the MEK/ERK inhibitors U0126 and PD98095 attenuated the TZD18 induced growth inhibition. In contrast, the MEK/ERK inhibitor U0126 did not suppress the up-regulation of CHOP and Bak/Bax induced by TZD18, indicating that the MEK/ERK pathway is not required for TZD18-induced expression of CHOP and Bak/Bax. How MEK/ERK participates in TZD18-induced growth inhibition of breast cancer cells is not understood. Recent studies have found that cytosolic retention of activated ERK1/2 is important for ERK-induced cell death (50). Future studies will investigate the location of activated ERK in TZD18-treated cells.

Clinical trials suggest that the genetic characteristics of breast cancer cells such as estrogen receptor status and overexpression of Her2 determine the efficiency of certain molecular therapeutics. In this study, different breast cancer cell lines with different genetic characters [estrogen receptor–positive, Her2 overexpressed, or triple negative (without expression of estrogen and progesterone receptors and Her2 amplification)] were used. The potency of TZD18 was not correlated with these genetic features. This observation suggested that the action of TZD18 on these cells was unrelated to estrogen- or Her2-initiated signaling. As showed above, the effects of TZD18 were mediated by endoplasmic reticulum stress response. To our knowledge, no data have been published to support a correlation between estrogen receptor status or Her2 overexpression and endoplasmic reticulum stress tolerance. Therefore, we were not surprised that all these types of breast cancer cells were, more or less, sensitive to the TZD18-induced growth inhibition. In contrast to breast cancer cells, we did not observe any obvious changes in the expression of GRP78, the general marker of UPR, as well as other UPR sensor proteins in the normal breast epithelial cell line MCF-10A after treatment with TZD18. This may explain why the MCF-10A cells are resistant to TZD18-induced endoplasmic reticulum stress.

In conclusion, we have shown in the present study that the novel PPARα/γ dual ligand TZD18 inhibited growth and induced apoptosis of breast cancer cells. Furthermore, our data suggested that cell death and/or growth arrest triggered by TZD18 was mediated by endoplasmic reticulum stress response, leading to activation of JNK, p38, MEK/ERK, and CHOP, which conspired to initiate cell death and/or growth inhibition. The more immediate cause of cell death may involve activation of the cell death receptor–related extrinsic and the Bak/Bax-associated intrinsic apoptotic pathways.

Disclosure of Potential Conflicts of Interest

No potential conflicts of interest were disclosed.

Acknowledgments

We thank Ms. Q. Guo from Merck (USA) for TZD18 and Ms. Liyan Hu and Ms. Tian Tian for their excellent technical assistance, as well as Mr. G. Adie for helping in the preparation of the manuscript.

References

1. Grimaldi PA. The roles of PPARs in adipocyte differentiation. Prog Lipid Res 2001;40:269–81.

2. Picard F, Auwerx J. PPAR(γ) and glucose homeostasis. Annu Rev Nutr 2002;22:167–97.

3. Straus DS, Glass CK. Anti-inflammatory actions of PPAR ligands: new insights on cellular and molecular mechanisms. Trends Immunol 2007;28:551–8.

4. Michalik L, Desvergne B, Wahli W. Peroxisome-proliferator-activated receptors and cancers: complex stories. Nat Rev Cancer 2004;4:61–70.

5. Krishnan A, Nair SA, Pillai MR. Biology of PPAR γ in cancer: a critical review on existing lacunae. Curr Mol Med 2007;7:532–40.

6. Elstner E, Mueller C, Koshizuka K, et al. Ligands for peroxisome proliferator-activated receptorgamma and retinoic acid receptor inhibit growth and induce apoptosis of human breast cancer cells *in vitro* and in BNX mice. Proc Natl Acad Sci U S A 1998;95:8806–11.

7. Elstner E, Williamson EA, Zang C, et al. Novel therapeutic approach: ligands for PPARgamma and retinoid receptors induce apoptosis in bcl-2-positive human breast cancer cells. Breast Cancer Res Treat 2002;74:155–65.

8. Fenner MH, Elstner E. Peroxisome proliferator-activated receptor-γ ligands for the treatment of breast cancer. Expert Opin Investig Drugs 2005;14:557–68.

9. Kim KY, Kim SS, Cheon HG. Differential anti-proliferative actions of peroxisome proliferator-activated receptor-γ agonists in MCF-7 breast cancer cells. Biochem Pharmacol 2006;72:530–40.

10. Posch MG, Zang C, Mueller W, Lass U, Von Deimling A, Elstner E. Somatic mutations in peroxisome proliferator-activated receptor-γ are rare events in human cancer cells. Med Sci Monit 2004;10:BR250–4.

11. Suchanek KM, May FJ, Robinson JA, et al. Peroxisome proliferator-activated receptor α in the human breast cancer cell lines MCF-7 and MDA-MB-231. Mol Carcinog 2002;34:165–71.

12. Liu H, Zang C, Fenner MH, et al. Growth inhibition and apoptosis in human Philadelphia chromosome-positive lymphoblastic leukemia cell lines by treatment with the dual PPARα/γ ligand TZD18. Blood 2006;107:3683–92.

13. Bocca C, Bozzo F, Martinasso G, Canuto RA, Miglietta A. Involvement of PPARα in the growth inhibitory effect of arachidonic acid on breast cancer cells. Br J Nutr 2008:1–12.

14. Saidi SA, Holland CM, Charnock-Jones DS, Smith SK. *In vitro* and *in vivo* effects of the PPAR-α agonists fenofibrate and retinoic acid in endometrial cancer. Mol Cancer 2006;5:13.

15. Liu DC, Zang CB, Liu HY, Possinger K, Fan SG, Elstner E. A novel PPAR α/γ dual agonist inhibits cell growth and induces apoptosis in human glioblastoma T98G cells. Acta Pharmacol Sin 2004;25:1312–9.

16. Zang C, Liu H, Waechter M, et al. Dual PPAR α/γ ligand TZD18 either alone or in combination with imatinib inhibits proliferation and induces apoptosis of human CML cell lines. Cell Cycle 2006;5:2237–43.

17. Gardner OS, Shiau CW, Chen CS, Graves LM. Peroxisome proliferator-activated receptor γ-independent activation of p38 MAPK by thiazolidinediones involves calcium/calmodulin-dependent protein kinase II and protein kinase R: correlation with endoplasmic reticulum stress. J Biol Chem 2005;280:10109–18.

18. Ron D, Walter P. Signal integration in the endoplasmic reticulum unfolded protein response. Nat Rev Mol Cell Biol 2007;8:519–29.

19. Kim R, Emi M, Tanabe K, Murakami S. Role of the unfolded protein response in cell death. Apoptosis 2006;11:5–13.

20. Szegezdi E, Logue SE, Gorman AM, Samali A. Mediators of endoplasmic reticulum stress-induced apoptosis. EMBO Rep 2006;7:880–5.

21. Zang C, Liu H, Posch MG, et al. Peroxisome proliferator-activated receptor γ ligands induce growth inhibition and apoptosis of human B lymphocytic leukemia. Leuk Res 2004;28:387–97.

22. Lin JH, Li H, Yasumura D, et al. IRE1 signaling affects cell fate during the unfolded protein response. Science 2007;318:944–9.

23. Melichar B, Konopleva M, Hu W, Melicharova K, Andreeff M, Freedman RS. Growth-inhibitory effect of a novel synthetic triterpenoid, 2-cyano-3,12-dioxoolean-1,9-dien-28-oic acid, on ovarian carcinoma cell lines not dependent on peroxisome proliferator-activated receptor-γ expression. Gynecol Oncol 2004;93:149–54.

24. Yamaguchi H, Wang HG. CHOP is involved in endoplasmic reticulum stress-induced apoptosis by enhancing DR5 expression in human carcinoma cells. J Biol Chem 2004;279:45495–502.

25. McCullough KD, Martindale JL, Klotz LO, Aw TY, Holbrook NJ. Gadd153 sensitizes cells to endoplasmic reticulum stress by down-regulating Bcl2 and perturbing the cellular redox state. Mol Cell Biol 2001;21:1249–59.

26. Janicke RU, Sprengart ML, Wati MR, Porter AG. Caspase-3 is required for DNA fragmentation and morphological changes associated with apoptosis. J Biol Chem 1998;273:9357–60.

27. Jiang CC, Chen LH, Gillespie S, et al. Inhibition of MEK sensitizes human melanoma cells to endoplasmic reticulum stress-induced apoptosis. Cancer Res 2007;67:9750–61.

28. Chen CL, Lin CF, Chang WT, Huang WC, Teng CF, Lin YS. Ceramide induces p38 MAPK and JNK activation through a mechanism involving a thioredoxin-interacting protein-mediated pathway. Blood 2008;111:4365–75.

29. Yoshida H, Matsui T, Yamamoto A, Okada T, Mori K. XBP1 mRNA is induced by ATF6 and spliced by IRE1 in response to ER stress to produce a highly active transcription factor. Cell 2001;107:881–91.

30. Lee AH, Iwakoshi NN, Glimcher LH. XBP-1 regulates a subset of endoplasmic reticulum resident chaperone genes in the unfolded protein response. Mol Cell Biol 2003;23:7448–59.

31. Thuerauf DJ, Morrison L, Glembotski CC. Opposing roles for ATF6α and ATF6β in endoplasmic reticulum stress response gene induction. J Biol Chem 2004;279:21078–84.

32. Luo S, Baumeister P, Yang S, Abcouwer SF, Lee AS. Induction of Grp78/BiP by translational block: activation of the Grp78 promoter by ATF4 through and upstream ATF/CRE site independent of the endoplasmic reticulum stress elements. J Biol Chem 2003;278:37375–85.

33. Harding HP, Novoa I, Zhang Y, et al. Regulated translation initiation controls stress-induced gene expression in mammalian cells. Mol Cell 2000;6:1099–108.

34. Yeh TC, Chiang PC, Li TK, et al. Genistein induces apoptosis in human hepatocellular carcinomas via interaction of endoplasmic reticulum stress and mitochondrial insult. Biochem Pharmacol 2007;73:782–92.

35. Kim SH, Hwang CI, Juhnn YS, Lee JH, Park WY, Song YS. GADD153 mediates celecoxib-induced apoptosis in cervical cancer cells. Carcinogenesis 2007;28:223–31.

36. Zinszner H, Kuroda M, Wang X, et al. CHOP is implicated in programmed cell death in response to impaired function of the endoplasmic reticulum. Genes Dev 1998;12:982–95.

37. Matsumoto M, Minami M, Takeda K, Sakao Y, Akira S. Ectopic expression of CHOP (GADD153) induces apoptosis in M1 myeloblastic leukemia cells. FEBS Lett 1996;395:143–7.

38. Kim DG, You KR, Liu MJ, Choi YK, Won YS. GADD153-mediated anticancer effects of N-(4-hydroxyphenyl)retinamide on human hepatoma cells. J Biol Chem 2002;277:38930–8.

39. Lei P, Abdelrahim M, Safe S. 1,1-Bis(3′-indolyl)-1-(p-substituted phenyl)methanes inhibit ovarian cancer cell growth through peroxisome proliferator-activated receptor-dependent and independent pathways. Mol Cancer Ther 2006;5:2324–36.

40. Sun SY, Liu X, Zou W, Yue P, Marcus AI, Khuri FR. The farnesyltransferase inhibitor lonafarnib induces CCAAT/enhancer-binding protein homologous protein-dependent expression of death receptor 5, leading to induction of apoptosis in human cancer cells. J Biol Chem 2007;282:18800–9.

41. Murakami Y, Aizu-Yokota E, Sonoda Y, Ohta S, Kasahara T. Suppression of endoplasmic reticulum stress-induced caspase activation and cell death by the overexpression of Bcl-xL or Bcl-2. J Biochem 2007;141:401–10.

42. Zong WX, Li C, Hatzivassiliou G, et al. Bax and Bak can localize to the endoplasmic reticulum to initiate apoptosis. J Cell Biol 2003;162:59–69.

43. Takeda K, Matsuzawa A, Nishitoh H, Ichijo H. Roles of MAPKKK ASK1 in stress-induced cell death. Cell Struct Funct 2003;28:23–9.

44. Wang XZ, Ron D. Stress-induced phosphorylation and activation of the transcription factor CHOP (GADD153) by p38 MAP Kinase. Science 1996;272:1347–9.

45. Zou W, Yue P, Khuri FR, Sun SY. Coupling of endoplasmic reticulum stress to CDDO-Me-induced up-regulation of death receptor 5 via a CHOP-dependent mechanism involving JNK activation. Cancer Res 2008;68:7484–92.

46. Dhanasekaran DN, Reddy EP. JNK signaling in apoptosis. Oncogene 2008;27:6245–51.

47. Thornton TM, Rincon M. Non-classical p38 map kinase functions: cell cycle checkpoints and survival. Int J Biol Sci 2009;5:44–51.

48. Arai K, Lee SR, van Leyen K, Kurose H, Lo EH. Involvement of ERK MAP kinase in endoplasmic reticulum stress in SH-SY5Y human neuroblastoma cells. J Neurochem 2004;89:232–9.

49. Joo JH, Liao G, Collins JB, Grissom SF, Jetten AM. Farnesol-induced apoptosis in human lung carcinoma cells is coupled to the endoplasmic reticulum stress response. Cancer Res 2007;67:7929–36.

50. Mebratu Y, Tesfaigzi Y. How ERK1/2 activation controls cell proliferation and cell death is subcellular localization the answer? Cell Cycle 2009;8.

Published OnlineFirst August 11, 2009; DOI: 10.1158/1535-7163.MCT-09-0347

Molecular Cancer Therapeutics

Induction of endoplasmic reticulum stress response by TZD18, a novel dual ligand for peroxisome proliferator-activated receptor α/γ, in human breast cancer cells

Chuanbing Zang, Hongyu Liu, Janina Bertz, et al.

Mol Cancer Ther 2009;8:2296-2307. Published OnlineFirst August 11, 2009.